# HEAT PUMP PROCESSES INDUCED BY LASER RADIATION

CR-166205
(R. G. Dickinson)

M. Garbuny and T. Henningsen

FINAL REPORT

(For Period Covering October 15, 1978 to April 30, 1980)

NASA-Ames
Contract No. NAS 2-10078

June 3, 1980




Westinghouse R&D Center
1310 Beulah Road
Pittsburgh, Pennsylvania 15235

# HEAT PUMP PROCESSES INDUCED BY LASER RADIATION

M. Garbuny and T. Henningsen

FINAL REPORT

(For Period Covering October 15, 1978 to
April 30, 1980)

NASA-Ames
Contract No. NAS 2-10078

June 3, 1980

Westinghouse R&D Center
1310 Beulah Road
Pittsburgh, Pennsylvania 15235

TABLE OF CONTENTS

# HEAT PUMP PROCESSES INDUCED BY LASER RADIATION

M. Garbuny and T. Henningsen
Westinghouse R&D Center
Pittsburgh, Pennsylvania 15235

## ABSTRACT

The construction of an experimental system has been completed for the demonstration of heat pump processes induced by laser radiation. Laser induced cooling of diatomic gases had been predicted as a result of a theoretical study under a previous NASA-Ames Contract NAS 2-9185. The system constructed on the present contract consists of a $CO_2$ laser, a frequency doubling stage, a gas reaction cell with its vacuum and high purity gas supply system, and provisions to measure temperature changes by pressure, or alternatively, by density changes. This report discusses the laboratory system constructed and the theoretical considerations for the choice of designs and components. The system is now ready for the measurement phase. However, for external reasons, such measurements will not be continued under NASA-Ames auspices.

## 1. INTRODUCTION: BACKGROUND AND MOTIVATION

The availability of lasers with increasing ratings of power delivery for various wavelength regions has made possible the application of coherent radiation to selective and nonselective processes of energy conversion. Such diverse fields as laser induced chemistry and isotope separation, nuclear fusion, machine operations and surgery have already benefited, or are expected to benefit, from the aspect of the laser as a power tool. The transmission of power from remote locations may be useful for certain topographic conditions and, in particular, for space applications. With this motivation, Westinghouse undertook a series of studies under contract with NASA-Ames to explore the feasibility and efficiency of remotely operating heating and cooling processes and the conversion of coherent radiation into mechanical energy.

The first study dealt with the concept of a thermal laser engine.[1] A beam from a remotely stationed power laser is focused into the working space of a heat engine through a suitable window such as zinc selenide or sapphire. A gas at resonance with the laser frequency absorbs the focused beam almost completely, reaches temperatures that may be well above 2,000°K, and performs work by expansion by one of several possible thermodynamic cycles. For optimized cycles of various absorbing gases admixed with helium, the study predicts[2] typical thermal efficiencies of 65%-75% at conservative temperatures. Subsequently small-scale versions of such laser engines have been built and successfully operated.[3] Further theoretical and design studies of thermal laser engines expanded on these ideas and arrived at predictions[4,5] of thermal conversion efficiencies as high as 90%.

The simple conversion of laser energy into heat in engine cycles can approach the Carnot efficiency characteristic of the operating temperatures used. Nevertheless, thermal laser engines utilize the coherence properties of the laser only in part. Because of the vanishing

entropy of coherent radiation,[6] thermodynamic considerations do not exclude the existence of engine processes with 100 percent conversion efficiency, if irreversible losses are ignored, such as those caused by friction. In other words, there is no need for the rejection of entropy and heat as in conventional thermal engines. Related thermodynamic arguments show that, just as mechanical work via compressors can be applied to heat pumps, coherent radiation can be used for remote cooling.

The exploration of such laser induced isentropic processes was the subject of a second NASA-Ames study contract.[7] This work showed[8] that there exists a very general method, called "resonance defect excitation", which represents an analog to mechanical heat pumps on the molecular level. In thermal equilibrium, the molecules of a gas assume a Boltzmann distribution over energy levels to which various degrees of freedom can contribute, such as translation, rotation, and vibration. If a photon raises a molecule from such a thermally generated state, $E_1$, to a higher level, $E_2$, the Boltzmann distribution will be reestablished, thereby cooling the environment by the amount $E_1$. As in a mechanical heat pump, the sum of the heat withdrawn and the entropy-free energy supplied is transferred to the gas. For purposes of cooling, this total energy is rejected either by radiation or by thermal relaxation after a certain decay time at which the gas may have been transferred to a heat sink structure. On the other hand, for purposes of energy conversion, the thermal relaxation of the gas may be used in an engine producing mechanical work. This is the case of a heat pump operating in series with a thermal engine. Ideally, the engine produces work with Carnot efficiency. The study[8] shows that operational conditions may be so adjusted that the heat rejected by the thermal engine is just equal to that withdrawn, and thus compensated, by the heat pump. Thermodynamics, of course, does not exclude the possibility of completely converting one form of entropy-free energy into another, even though intermediate heat processes are involved.

Because of unavoidable losses and other irreversible processes, 100% conversion efficiency from laser radiation into work can not be

attained. Furthermore, the operational conditions for such ideally complete conversion pose rather stringent practical requirements. Nevertheless, laser engines incorporating a heat pump process may have important advantages, even if the optimum conditions are only partially obtained. Rather high efficiencies can be obtained at much lower temperatures than those required for the simpler thermal laser engines, with a resulting reduction of thermal stresses. Gas kinetic cooling by laser radiation, of course, is of interest in its own right. A capability of remotely cooling an isolated component, such as a detector array, with powers promising to exceed those produced with thermoelectric devices, may have important applications. Not the least of its advantages is that laser induced cooling can reduce substantially the gas temperature in nanoseconds and reach a steady state within a fraction of a second. Critical chemical and other reactions in gases may be controlled by such processes with speeds not available by other measures.

Perhaps the most suitable resonance process for a laser heat pump uses thermally excited rotational states of diatomic gases as starting points $E_1$. Although we had independently proposed this method initially for quasi-isentropic laser engines, other laser induced gas kinetic cooling processes were proposed and, in part, demonstrated. These processes use either translational energy or vibrational energy as starting levels $E_1$. Translational cooling[9] can reduce the temperature of atoms[10] or ions[11] to well below 1°K but, for inherent reasons, only in very small quantities ($<10^5$ particles). Vibrational cooling[12,15] can operate on large quantities of gas, but achieves a temperature reduction typically of only a fraction of a degree. Rotational cooling produces an action intermediate between these two extremes. It can cool gases in amounts limited only by the available laser power and, starting from room temperature or above, to a predicted[8] range between liquid helium and nitrogen.

The construction of equipment and measurements for the demonstration of rotational cooling were the subject of the current contract with NASA-Ames. This report describes design analysis and the completed

equipment construction for laser induced cooling of carbon monoxide-nitrogen mixtures, the point reached at the end of the present contract period. Although the broad theory of cooling initiated by laser radiation has been described in the referenced reports and papers, a brief and simple description of the relevant features is presented in Section 2 so as to provide the basis for the design considerations involved.

The equipment is at present ready for the measurement phase. While this work was in progress, the group interested in this field was reorganized for activities in other departments, and the contract monitor left NASA-Ames. For this reason, by request of NASA-Ames, the measurement phase of this program will not be continued under NASA-Ames sponsorship.

## 2. THEORETICAL CONSIDERATIONS

This section presents a short review of the theory underlying molecular rotational cooling by defect resonance radiation and discusses the resulting optimal choice of target gases and their mixtures.

Consider a gas containing N molecules. In thermal equilibrium at a temperature T, the N molecules assume the Boltzmann distribution[14]

$$n_i = g_i A\, e^{-E_i/kT} \quad . \tag{1}$$

Here $E_i$ represents the total energy (quantized) of a molecule in the level i, to which all degrees of freedom contribute that make up the specific heat of the gas, viz., translation, rotation, and vibration; $n_i$ is the number of molecules of energy $E_i$; $g_i$ is the statistical weight of level i (i.e., the number of states with the same energy $E_i$) and A is a constant obtained from the condition that the sum of all $n_i$ equal N. The solid curve in Fig. 1 represents the Boltzmann distribution in the form $E_i(n_i)$, i.e., the abscissae measure the populations of various energy levels. The statistical weights $g_i$ are, for simplicity, set equal to unity in this graph.

Figure 1 further shows three discrete energy levels, $E = 0$, $E = E_1$, and $E = E_2$. $E = 0$ represents the lowest energy (ground state) which the molecule can assume, i.e., its vibrational and rotational quantum numbers are, respectively, $v = 0$ and $J = 0$, and its translational energy (with respect to the observer) is zero. $E_1$ is a rotational level of the vibrational ground state ($v = 0$). $E_2$ is the rotational ground state ($J = 0$) of the first excited vibrational level ($v = 1$). Here we ignore the fact that translational energies should be added to $E_1$ and $E_2$. Although rotational and translational energies are of the same order (several hundred $cm^{-1}$ in spectroscopic units at room temperature), the change of translational energy in emission and absorption is very small in comparison because of the small momentum of the photon. The

Curve 722777-A

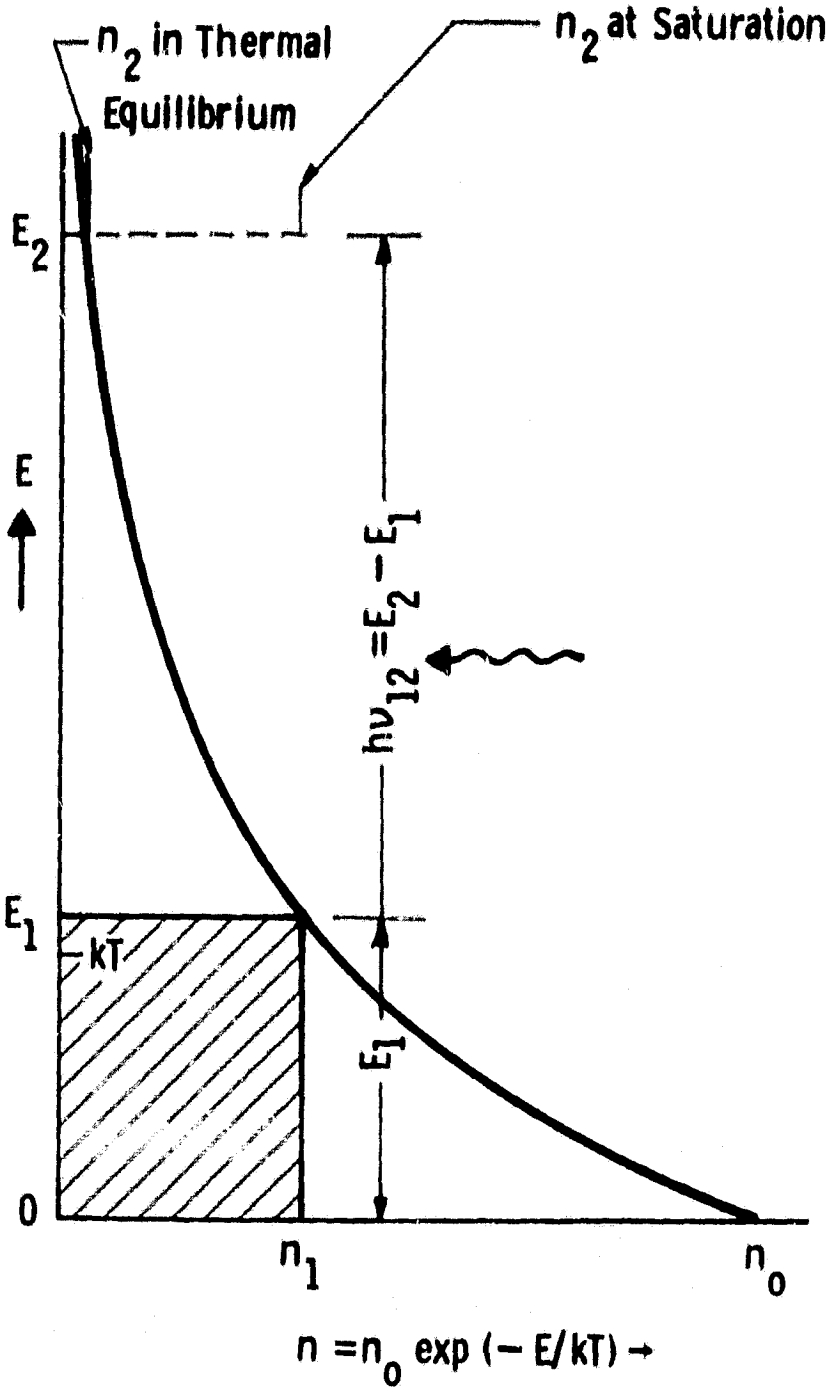


Fig. 1. Origin of radiative cooling by defect excitation as shown for a system of three levels with equal statistical weights. Shaded area represents approximately heat withdrawn at constant temperature for a saturating excitation.

frequency $\nu_{02}$ of a photon with energy $h\nu_{02} = E_2$ is at resonance with the fundamental (first harmonic) vibration of the molecule.

Assume that the molecule finds itself in the thermally excited state $E_1$ representing the first rotational state (i.e., $J = 1$) of the vibrational ground state. The transition from $E_1$ to $E_2$ can now be excited by a photon of energy $h\nu_{12} = E_2 - E_1$, the "defect" $E_1$ being made up by heat energy. Subsequent events affecting the heat balance depend on the various rates of energy transfer. These thermal relaxation rates are, to a major extent, dominated by molecular collisions for which certain general relationships exist valid for most gases. Exchange of translational energy of two molecules occur at every collision and so do exchanges of rotational energy and also exchanges between translational and rotational energy. The molecules of a gas at 300°K and 100 Torr (corresponding to a density of $3 \cdot 10^{18}$ molecules/cm$^3$) each undergo $10^9$ collisions per second, i.e., the translation-rotational (T-R) relaxation times are in the order of $10^{-9}$ sec. Thus the defect excitation of the molecule from $E_1$ to $E_2$ cools the translational-rotational heat reservoir by $E_1$ in $10^{-9}$ sec. The vibrational energy $E_2$ can also relax thermally by its transfer to translational or rotational energies (V-T-R), but usually at much slower rates. In a few diatomic gases, such as CO and $N_2$, only one in $10^9$-$10^{10}$ collisions produces thermal (V-T-R) relaxation. Thus, whereas $E_1$ is withdrawn as heat in $10^{-9}$ sec, $E_2 = h\nu_{12} + E_1$ is returned as heat only after several seconds. Under these conditions, CO relaxes from $E_2$ much faster by radiation owing to a spontaneous emission lifetime of 30 msec. If conditions can be so arranged that in the average an energy $E_2$ is carried away by radiation, continuous defect excitation produces continuous cooling. If, on the other hand, the CO radiation is absorbed by the walls, cooling will occur over several seconds until diffusion to and from the walls reverses the process.

The choice of the level $v = 0$, $J = 1$ represents the simplest case of CO cooling by laser. Figure 2 shows, on its left side, the energy term scheme of CO for the first and second vibrational level. The rotational energy of a state with quantum number J is given by[15]

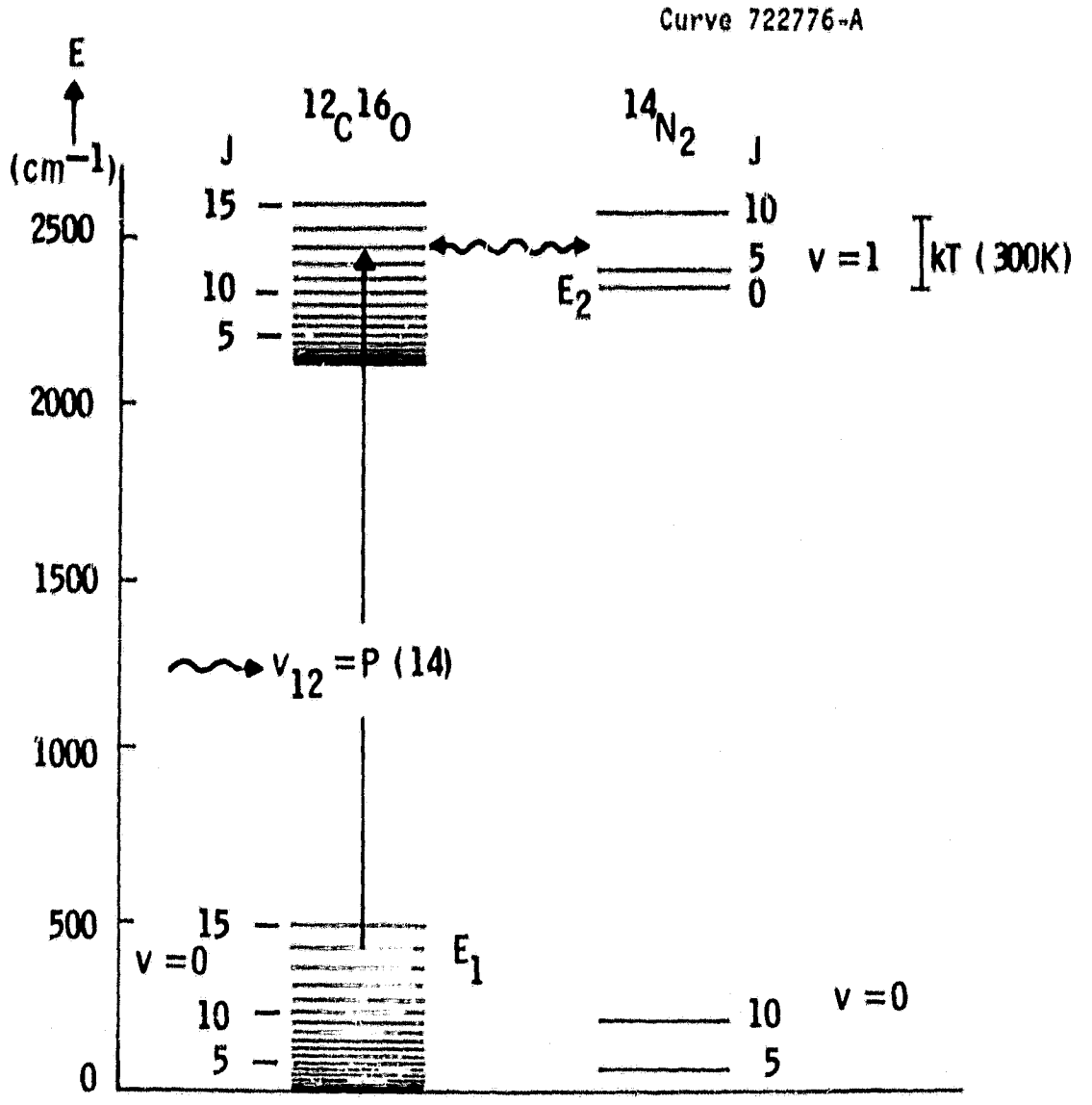


Fig. 2. Vibrational-rotational energy term schemes for CO (left) and $N_2$ (right). Transitions from v = 0 to v = 1 will produce gas cooling, if simultaneously the rotational energy changes from higher to lower values. In pure CO cooling is initiated by P-transitions such as the indicated P(14) absorption. Larger rotational energy defects and hence larger cooling is predicted for mixtures of CO with $N_2$. Here, the energy of the v = 1, J = 13 state of CO is transferred by resonance collision (wavy line) to a low lying J-state of the $N_2$ level v = 1.

$$E_{rot} = J(J+1)B_v \qquad (2)$$

where $B_v$ is the rotational constant for the energy state given by v and J. The height of the J-state above the respective J = 0 state in Fig. 2 is a measure of $E_{rot}$.

Quantum selection rules limit transitions in diatomic gases to the condition $\Delta J = \pm 1$. Transitions of the type J→J+1 (R-lines) add rotational energy; transitions of the type J→J-1 (P-lines) reduce the rotational energy of the molecule. The rotational energies of the v = 1 level thermalize with the translational-rotational heat reservoir about as fast as those of level v = 0. Therefore the amount of net heat withdrawn per molecule excitation in the cooling P-transitions is obtained from Eq. (2) as

$$\Delta E_{rot} = J(B_o+B_1) + J^2(B_o-B_1) \quad . \qquad (3)$$

The cooling effect per molecule transition increases therefore for P(J) transitions with increasing J. Because $B_o$ is only slightly larger than $B_1$, $\Delta E_{rot}$ is approximately proportional to J, for large J.

If $n_p$ photons are absorbed by gas molecules in the $E_1$ level, the heat withdrawn is $n_p \Delta E_{rot}$. Note that $n_p$ is limited by saturation. If the pumping rate from $E_1$ to $E_2$ is larger than the relaxation rate from level $E_2$, the population $n_2$ in $E_2$ will increase to a value that, with respect to the population $n_1$, has the ratio of the respective statistical weights:

$$n_2/n_1 = g_2/g_1 \qquad (4)$$

at which point that gas becomes transparent (because of the balancing stimulated emission) to radiation at $\nu_{12}$. In Fig. 1, the population limit $n_2$ is indicated by a horizontal bar for the case $g_2 = g_1$ or $n_2 = n_1$. Because of the fast thermalization of the rotational states, the rotational manifold of the v = 1 level is quickly filled, subject to

conditions (1) and (4). The number $n_p$ of defect excitations up to the point of saturation is therefore larger than $n_2$ by a factor C equal to the ratio of the total population of the rotational manifold to that in the particular J-state at $E_2$.

To assess the magnitude of cooling available from P-transition cooling, consider the effect of CO irradiation at the frequency of its P(14) line (v = 0, J = 14→v = 1, J = 13). With $B_o = 1.923\ cm^{-1}$ and $B_1 = 1.905\ cm^{-1}$, Eq. (3) yields $E_{rot} = 57.12\ cm^{-1}$, corresponding to $113.5 \cdot 10^{-16}$ erg, per transition. If driven to saturation, about half of all CO molecules have undergone the P-transitions so that, in the average, $56.8 \cdot 10^{-16}$ erg, i.e., about 5.5% of the heat content (2.5 kT/molecule) at 300 K has been withdrawn from the translational-rotational heat reservoir. The molecules in the v= 1 level, of course, relax to the vibrational ground level with a certain time constant. They thereby provide a fresh supply for repeated cooling events as long as much of this relaxation is non-thermal by the average effect of spontaneous P- and R-line emissions.

The P-transitions extract only the difference $\Delta E_{rot}$ of rotational energy in the two vibrational levels. However, it is possible to extract all (or at least the major part) of the energy $E_{rot}$ given by Eq. (2) by collisional energy transfer to a second gas, such as $N_2$ (see Fig. 2). The rotational ground state of $N_2$ of the v = 1 level has an energy which is $187.5\ cm^{-1}$ higher than in CO. That $N_2$ ground state is, however, virtually (within about $10\ cm^{-1}$) at resonance with the J = 10 or J = 9 states of the v = 1 level of CO. Excited, for example, by radiation at the frequency of P(10), the CO state at J = 9 (i.e., $E_2$) can transfer its energy very fast to $N_2$. This defect excitation of $N_2$ occurs at the expense of the energy $E_1$, viz., $J(J+1)B_o$. With J = 10, this energy equals $E_1 = 211.5\ cm^{-1}$ per molecular excitation, considerably larger than $\Delta E_{rot} = 57.1\ cm^{-1}$ of the P(14) transition.

The gas mixture may contain, typically, 10 Torr CO and 150 Torr $N_2$. Excitation of the P(10) transition is expected to be distributed over the rotational manifolds of the v = 1 levels in both gases within less than $10^{-7}$ seconds, while the manifolds in the v = 0 level are

correspondingly depleted. The detailed calculation[8] shows that, if N molecules of the mixture are brought to saturation, the heat withdrawn from the translational-rotational reservoir is approximately

$$\Delta H = n_p E_1 \approx \frac{(2J-1)E_1 e^{-E_1/kT}}{1+(2J-1)e^{-E_1/kT}} N \qquad (5)$$

where J is the rotational quantum number of the initial state of the transition (J = 10 in this example) and $E_1 = J(J+1)B_o$. Equation (5) is valid for isothermal operation, i.e., by withdrawal of heat at constant temperature T from a heat reservoir in thermal contact with the gas. The equation is also valid for adiabatic operation in which a gas mass, thermally isolated from any walls, is cooled from a temperature T' to a lower temperature T so that (for constant specific heat $c_v$) $T'-T = \Delta H/c_v$.

Inspection of Eq. (5) shows that for a given T, the energy $E_1$ assumes an optimum value for which $\Delta H$ is a maximum. The physical reason for this is that, while the heat withdrawn equals $E_1$ in each transition, the population in $E_1$ decreases exponentially, as $E_1$ increases, with a resulting reduction of the possible number of such transitions according to Eqs. (1) and (2). By the same argument, there exists a temperature T for a given $E_1$, at which the entropy transfer $\Delta H/T$ is a maximum. In adiabatic cooling, this optimum temperature for fixed $E_1$ also defines the maximum of a cryogenic merit factor $M = (T'-T)/T$. M is the relative temperature reduction produced by the number $n_p$ of photons sufficient for saturation.

In P(10) transition cooling of the $CO/N_2$ mixture, with $E_1$ fixed at 211 $cm^{-1}$, the optimum temperature is 121°K. Pumping to saturation extracts 61% of the thermal energy of the gas at that temperature in isothermal operation. The predicted adiabatic cooling effect with P(10) irradiation is represented in Fig. 3. Starting at 730°K, the gas temperature decreases almost linearly with irradiation time, scaled in units of the (radiative) relaxation time $\tau_{E_2}$. The merit factor $\Delta T/T$ reaches the maximum of 61% when the gas temperature passes through 121°K.

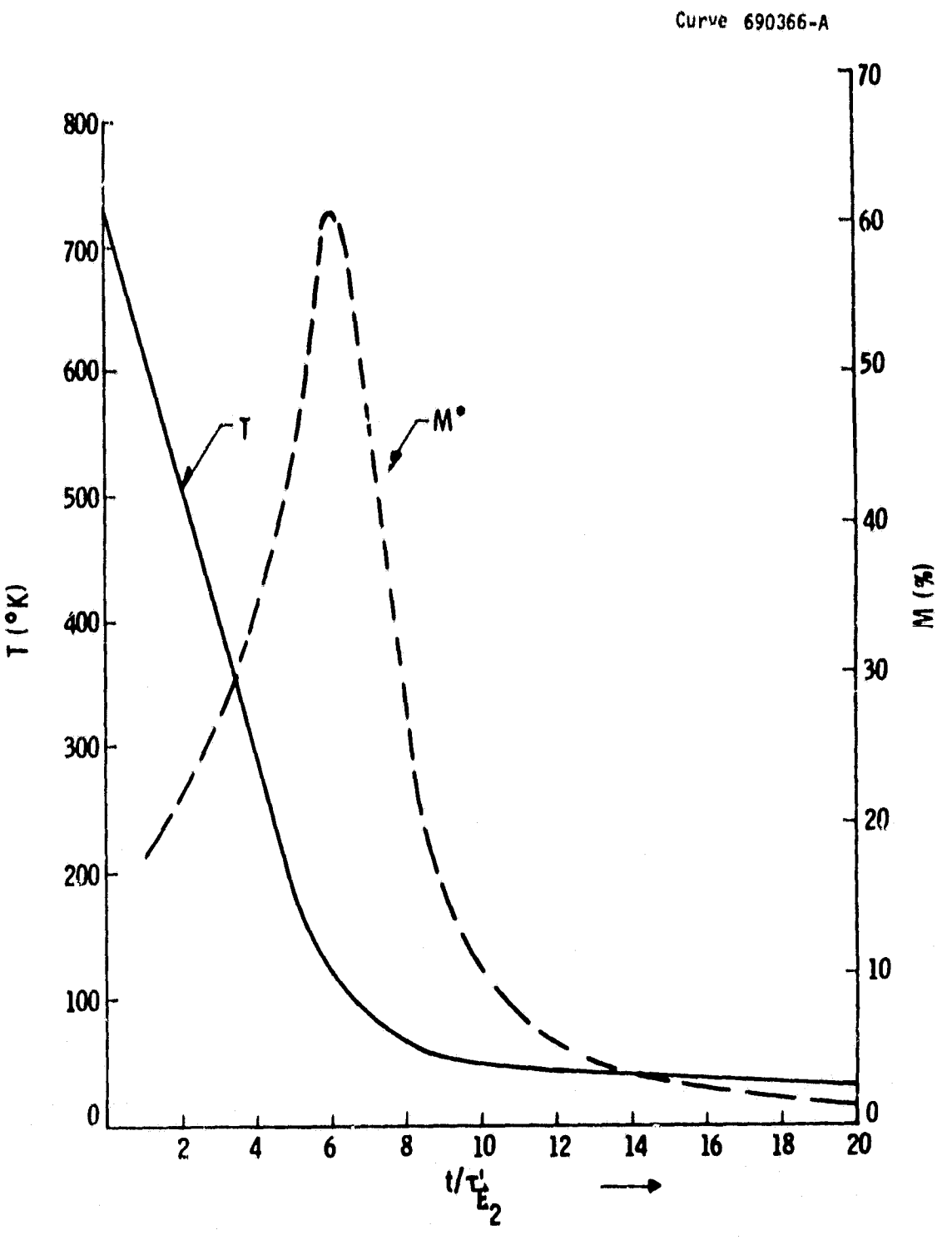


Fig. 3. Adiabatic cooling of $^{12}C^{16}O/^{14}N_2$ mixture by a radiation pulse of a duration long compared with the time $\tau_{E_2}$ during which the ground state population is being renewed mainly by radiative relaxation. The curve for $M^* = \Delta T/T$ represents the relative temperature decrease as a function of time t during each interval $\tau_{E_2}$.

## 3. CHOICE OF EXPERIMENTS

Studies of the adiabatic and isothermal types of laser induced cooling are equally of interest in terms of the knowledge to be gained of the gas kinetic processes involved and possible applications at a later time. However, adiabatic experiments are simpler to perform and should precede isothermal studies. In heat pump processes there is always a stage in which the heat withdrawn, in addition to the entropy-free energy added, must be rejected. In the radiative heat pump process, the translational-rotational heat content and gas temperature is reduced within a time as small as $10^{-9}$-$10^{-10}$ sec, unless simultaneously heat is injected. The energy stored in the vibrational levels is released in two ways. First, spontaneous emission carries away, in the average of P- and R-transitions, the radiation energy injected and the T-R heat withdrawn. This process has, for example, a time constant of 30 msec in pure CO, but is prolonged by a factor equal to the ratio of $N_2$:CO concentrations in the mixture. Second, the energy stored in the vibrational levels may be converted into heat by VTR collisions among the molecules or by collisions of molecules with the walls to which they diffuse. For CO and CO/$N_2$, these destructive processes have time constants from 1-10 sec. Thus the rate of cooling events far exceeds that of heating. In adiabatic operation, the laser beam may pass through the core of a stagnant gas in a cylindrical container with walls which absorb spontaneously emitted radiation and are maintained at a certain temperature $T_w$. The core of the gas will then have a temperature which, starting at $T_w$, will have the type of reduction shown in Fig. 3. The measurement of the temperature-time behavior is relatively simple and, aside from testing the validity of the theoretical predictions, throws light on secondary processes such as on vibrational escalation to be discussed at the end of this report.

Isothermal cooling requires that the translational and rotational states of the gas are strongly coupled to a heat reservoir at constant temperature, while the vibrational states remain isolated from it. The realization of such provisions is possible, or at least conceivable, in a surprising number of ways. However, all these methods are more complex than the adiabatic measurements and were, therefore, not considered for the present project.

## 4. LASER SYSTEM FOR THE DEFECT EXCITATION OF CO(v=0)→(v-1) TRANSITIONS

### 4.1 Compatibility Requirements

Various diatomic molecules have an ionic (vibrational) dipole moment, hence an infrared spectrum, and also a rate of spontaneous emission which exceeds their (VTR) rate by many orders of magnitude. Among these, CO was chosen as the cooling medium because it has the smallest (VTR) decay rate and therefore is most suitable for the detailed study of the other molecular energy transfer mechanisms involved. CO can also serve as "collisional pump" source for the excitation of other diatomic gases, such as $N_2$, which have a very small (VTR) rate, but lack an ionic dipole moment. (VTR) rates are, as are collision mechanisms, proportional to pressure; but for a number of reasons, notably diffusion to the walls, the optimum pressure is typically about $10^2$ Torr.

The pressure has an important bearing on the optical properties of the gas and the selection of the laser source. Self-broadening[16] of the P(10) line in the fundamental band of CO amounts to about 0.075 $cm^{-1}$ $atm^{-1}$ (HWHM) at 300 K. The line width varies as $T^{-0.7}$ and decreases[17] slowly for increasing J. Somewhat smaller values are obtained for $CO/N_2$ mixtures. Thus for maximum absorption the pumping laser frequency must be tuned to CO molecules at 100 Torr within 0.01 $cm^{-1}$.

The fraction $P_{abs}/P_o$ of laser power P absorbed by a path length L of the gas is up to certain intensities given by

$$P_{abs}/P_o = 1 - e^{-\sigma(\nu)nL} \qquad (6)$$

where $\sigma(\nu)$ is the absorption cross section and n the gas density. The absorption cross section, measured with the nearly monochromatic radiation of a laser at the peak of the absorbing line, $\nu_o$, varies inversely with the line width of the absorber. At the peak of the strong P-lines

in the fundamental CO band, a cross section of $63 \cdot 10^{-18}$ $cm^2$ was measured[18] for a linewidth of 0.0024 $cm^{-1}$ (Doppler limit), whereas the cross section for CO in atmospheric air is given[19] as $1.8 \cdot 10^{-18}$ $cm^2$ for a linewidth of 0.07 $cm^{-1}$. At a 100 Torr CO pressure, the peak cross section is therefore expected to be about $15 \cdot 10^{-18}$ and about 7-8% larger for CO admixed to $N_2$. Equation (6) shows then that radiation at peak resonance traversing through 100 Torr CO will be 95% absorbed over a length L = 0.057 cm, and over L = 0.53 cm in the $N_2$ gas mixture containing 10 Torr CO. However, in intense laser beams, $\sigma(\nu)$ quickly decreases towards zero as the v = 1 level of CO saturates (the rotational states thermalizing by collisions) and stimulated emission balances absorption processes. Therefore the beam continues in its path, bringing successive sections of CO to transparency ("saturation wave").

For the choice of a suitable laser source, it is important to know the extent to which its frequency can deviate from a peak resonance at a frequency $\nu_o$ and still provide sufficient excitation of the gas. Since the dominant process of line broadening at the prospective CO pressures is self- and collision-broadening, the cross section $\sigma(\nu)$ has the Lorentzian spectral profile

$$\sigma(\nu) = \frac{(S/\pi)\gamma}{(\nu-\nu_o)^2 + \gamma^2} \qquad (7)$$

where the normalization factor $S = \int_{-\infty}^{\infty} \sigma(\nu)d\nu$ and $\gamma$ is the (HWHM) linewidth. It is seen from Eq. (7), that if the laser frequency $\nu$ is displaced from peak resonance $\nu_o$ by $5\gamma$ or $10\gamma$, the path length L has to be increased by 26 or 101, respectively, to achieve the absorption effects at peak resonance described in the preceding paragraph, according to Eq. (6). Thus a cell containing 100 Torr CO must have a length of at least 1.5 cm or, respectively, 5.8 cm to produce 95% absorption. The corresponding lengths for $CO/N_2$ are 14 cm and 53 cm.

## 4.2 Alternatives for the Laser System

Since CO lasers produce large powers with high efficiencies, they would provide the most perfect solution for the radiation source problem, provided they could yield sufficient powers in the 1-0 band. However, only a few 1-0 lasers have been built,[20] and they provide only low powers.[21] Single-line CO lasers for the 1-0 band yielding larger powers can be built, but the effort presents a project in itself.

Continuously tunable infrared lasers can also provide a perfect match in frequency, albeit again at low spectral radiances. An exception perhaps is the $LiNbO_3$ parametric tunable laser which, however, can only reach the overtone 2-0 band of CO. The resulting low absorbance over, typically, 12 cm would then have to be compensated by multiple reflections through the gas cell.

A third class of resonance radiation sources for CO is comprised of lasers with lines which directly, or via SHG or other parametric conversion (e.g., Raman shift), coincide with the fundamental absorption lines of CO. In fact, frequency doubling of $CO_2$ laser lines has been used for various purposes with the coincidences shown in Table I.

**TABLE I**

| $CO_2$ transition (001)-(020) | Doubled $CO_2$ freq. in $cm^{-1}$ | CO transition | CO frequency $cm^{-1}$ | $\Delta\nu$ $cm^{-1}$ |
|---|---|---|---|---|
| P(24) | 2086.326 | P(14) | 2086.323 | 0.003 |
| R(18) | 2154.605 | R(2) | 2154.598 | 0.007 |
| R(30) | 2169.270 | R(6) | 2169.200 | 0.070 |

For the planned experiments, the first of these coincidences had to be chosen because of the type of transition and the excellent overlap even at CO or $CO/N_2$ pressures well below 100 Torr. $Tl_3AsSe_3$ (TASS, developed at Westinghouse), proustite, and $CdGeAs_2$ all qualify as $CO_2$ frequency doubling crystals. Among these, $CdGeAs_2$ excels in SHG efficiency by more than an order of magnitude.[22] It turned out that only one source, viz., a

group at MIT Lincoln Laboratories, was growing and demonstrating $CdGeAs_2$ crystals of sufficient size and quality to provide a SHG output power level useful for our experiments.

Before committing ourselves to any laser system, we undertook a search and calculation to find direct line coincidences between lines of known lasers of sufficient power and CO. Unfortunately, the fundamental CO spectrum coincides with strong laser lines of other media only in one case, viz., its P(22) transition at 2050.86 $cm^{-1}$ with the krypton laser line at 2050.86 $cm^{-1}$. However, another possibility is a match between $^{12}C^{16}O$ lasers and the fundamental absorption band of a heavier CO isotope. The band spectra lasing in the former between higher vibrational levels occupy successively longer wavelength regions and can therefore be expected to overlap the fundamental band of some CO isotopes shifted to longer wavelengths by the larger mass of the vibrating ions. We derived, therefore, the P-line spectrum of suitable CO isotopes from recently published Dunham coefficients.[23] The $^{12}C^{16}O$ laser frequencies were obtained from the most recent tables[20] of CO (vacuum) wavelengths. The search for coincidences yielded the results shown in Table II.

TABLE II

| $^{12}C^{16}O$ Laser Transition | | | CO Isotope Transition | | | |
|---|---|---|---|---|---|---|
| v'→v" Terms | Comb. | Freq. ($cm^{-1}$) | P-Line | | 0-1 Band Freq. ($cm^{-1}$) | Δν $cm^{-1}$ |
| 3-2 | P(16) | 2025.876 | $^{13}C^{18}O$ | P(5) | 2025.9281 | 0.052[1] |
| 5-4 | P(6) | 2015.0029 | " | P(8) | 2014.9121 | 0.0908 |
| 5-4 | P(7) | 2011.0911 | " | P(9) | 2011.1813 | 0.0905 |
| 3-2 | P(18) | 2017.2136 | $^{12}C^{18}O$ | P(19) | 2017.1349 | 0.0787 |
| 3-2 | P(14) | 2012.8338 | " | P(20) | 2012.8801 | 0.0463 |
| 4-3 | P(14) | 2008.5552 | " | P(21) | 2008.5955 | 0.0435 |
| 4-3 | P(15) | 2004.3369 | " | P(22) | 2004.2811 | 0.0558 |

The accuracy of the isotope frequency calculations should be within 0.0020 $cm^{-1}$. To test the reliability of this estimate, published Dunham[23] coefficients were used to determine the $^{12}C^{16}O$ P-line spectrum of the fundamental band up to the fourth order of the quantum state terms, just as had been done for the CO isotopes. These calculated frequencies were then compared with those measured in $^{12}C^{16}O$ and published in recent laser tables,[20] as well as with CO (vacuum) wavelength standards[24] established before 1966. We found that the calculated frequencies agreed within better than 0.0002 $cm^{-1}$ with the former and within 0.002 $cm^{-1}$ with the latter. The older standards, of course, were limited in accuracy by Doppler line broadening and by a larger error limit for the speed of light. We conclude that the coincidence predictions are accurate to a degree better than that required.

The best overlap between (v'-v") transitions of $^{12}C^{16}O$ and (1-0) of a CO isotope should occur for $^{14}C^{18}O$. Unfortunately, the spectrum of the latter cannot be determined with sufficient accuracy at present, and the availability of the gas is in question.

At a 100 Torr gas pressure, the P-lines of CO have a linewidth of about 0.01 $cm^{-1}$. The mismatch of their coincidences with doubled CO frequencies, shown in the last column of Table II, produces gaps from four to nine times the linewidth at 100 Torr. According to the preceding section, therefore, most of the laser radiation is absorbed, even in the least favorable combination of gas mixtures and exciting lines, in gas cells of convenient size.

The rotational ground state of the v = 1 level in $^{12}C^{16}O$ lies 99.58 $cm^{-1}$ above that of $^{13}C^{18}O$. Therefore, a mixture of the two isotopes, typically of 10% $^{13}C^{18}O$ and 90% $^{12}C^{16}O$ provides a suitable medium for rotational cooling, the energy term scheme being quite similar to that of Fig. 2. The predicted adiabatic cooling process[8,25] has a trend similar to that shown in Fig. 3. The rotational constant $B_1$ of $^{13}C^{18}O$ equals 1.73 $cm^{-1}$ so that, according to Eq. (2), the (v = 1, J = 7) state of this isotope is in near resonance with the (v = 1, J = 0) state of $^{12}C^{16}O$. The proper defect excitation is therefore provided by the P(8) transition of that isotope which, with $B_o$ = 1.75 $cm^{-1}$, starts at

$E_1$ = 125.74 $cm^{-1}$. Excitation of that line is possible with the coincidence shown in the second row of Table II. The predicted adiabatic cooling process in the CO isotope mixture has its peak efficiency at 75 K and reaches 24 K asymptotically.

The coincidences of $^{12}C^{16}O$ laser frequencies with P- lines of $^{12}C^{18}O$ cover the range J = 19 to J = 22 of the latter. The location of these lines yields relatively high values for P-transition cooling of pure $^{12}C^{18}O$. Furthermore, they reach energies sufficient for transfer to the v = 1 level of $N_2$.

In summary, a line-tunable CO laser provides coincidences with CO isotopes suitable for experiments with P-line cooling in CO and transfer cooling in $CO/N_2$ and CO isotope mixtures. None of the other methods mentioned before exhibit this flexibility.

### 4.3 Choice and Acquisition of the Laser System

Although the analysis described in the preceding section had indicated that CO laser pumping of CO or CO mixtures represented the best choice, a decision had to be made on the basis of cost in view of the limited scope of this project. Cost considerations excluded the purchase of a commercial CO laser dedicated to this project. The operation of CO lasers with upper vibrational levels $v' \leq 6$ requires cooling to at least 130 K. A survey of CO lasers not in present use discovered a few that were available, but none capable of delivering the transitions shown in the third column of Table II (or transitions with less favorable coincidences not listed there). Cost consideration also excluded acquisition of a krypton laser for the coincidence with the P(22) absorption line of CO.

It was therefore necessary to pursue the next best option, viz., the combination of $CO_2$ laser and $CdGeAs_2$ SHG crystal. The (0-1) P(14) line of $^{12}C^{16}O$, within the Doppler linewidth coincident with the frequency doubled P(24) line in the (001)-(020) band of $CO_2$, excites CO to an energy somewhat above the (v = 1, J = 0) state of $N_2$. However, the slightly decreased resonance transfer efficiency of this process compared

to P(10) operation is amply compensated by increased net energy defect exchange. The cooling effect of the P(14) transition in pure CO is, of course, relatively favorable, as described in Section 2.

We received from Dr. Mooradian's group at the MIT Lincoln Laboratories a $CdGeAs_2$ crystal of approximate dimensions 3 x 3 x 3 mm. According to a communication from Dr. Menyuk, attempts to achieve output powers of 1 watt had to be limited to pulsed operation. To reduce absorption by the crystal of the pump radiation, the crystal is cooled by contact with a liquid nitrogen reservoir.

Several $CO_2$ lasers, operating either continuously or pulsed were available at the Westinghouse R&D Center. Among these, a longitudinal discharge laser was chosen and installed in the system. It has a maximum output power rating of 200 watts cw, but can be operated pulsed at lower average powers. At any rate, however, a lower power limit is imposed by the $CdGeAs_2$ crystal.

The crystal is supported in a metal dewar equipped with NaCl windows. Because of the small size of the crystal, we acquired a beam condenser which reduces the diameter of the laser beam to about 2.5 mm.

## 5. THE GAS KINETIC REACTION CELL

In view of the power limitation of the source, enforced by the limited radiation damage threshold of the small SHG crystal, the design of the cell containing CO or $CO/N_2$ had to be a compromise of mutually conflicting requirements. The diameter of the cell had to be small enough so that the adiabatic temperature reduction produced in the path of the 2.5 mm dia. laser beam would be easily measurable by the resultant pressure reduction. However, the cell diameter has also to be large enough so that the diffusion time of the vibrationally excited molecules to the walls was large compared to the time of vibrational energy relaxation by spontaneous emission. Similar trade-offs apply to the choice of the gas pressure. Too small a pressure decreases the diffusion time of the vibrationally excited molecules to the walls to magnitudes no longer large compared with those of radiative relaxation. Too large a pressure, however, decreases the (VTR) time constant of thermal relaxation to a point at which spontaneous emission is no longer the dominant relation mechanism. The optimal choice of the cell length depends on the CO pressure (or rather on its molecular density) and on the available laser power. The number N of molecules in the path of the laser beam equals the product of the molecular density n, the beam cross section, and the cell length. Obviously for optimal operation, the number N should be just large enough to deplete the available beam power by absorption. However, a possibly conflicting consideration is that the length should also be large enough to allow the flexibility needed for a variety of experiments, involving different gas mixtures, densities, temperatures, and laser powers.

The design of the gas reaction cell was based on all these considerations which are outlined in the following in greater detail.

## 5.1 Power Balance and Cell Dimensions

In the adiabatic cooling process of $CO_2/N_2$, the temperature undergoes initially an almost linear descent and then approaches a lower limit asymptotically. After the onset of laser radiation, the population in the $v = 1$ levels is built up close to the saturation point of CO by $n_p$ photons of energy $h\nu_{12}$ ($= E_2 - E_1$). The $n_p$ molecules in the $v = 1$ levels now decay at a rate $1/\tau_{E_2}$ mainly because of spontaneous emission. To maintain the excited population close to the saturation value, the laser system must therefore supply the pump power

$$P = n_p h\nu_{12}/\tau_{E_2} \quad . \tag{8}$$

However, $n_p$ is a function of temperature since the saturation population in $E_2$ has to adjust to population in $E_1$ which decreases with falling temperature. Introducing $n_p = \Delta H/E_1$ from Eq. (5) into Eq. (8), we obtain

$$P = ALnh\nu_{12} \frac{(2J-1)e^{-E_1/kT}}{1 + (2J-1)e^{-E_1/kT}} \cdot \frac{1}{\tau_{E_2}} \tag{9}$$

where the number N of molecules in the path of the laser beam has been expressed as the product of beam area A, cell length L and molecular density n. We now choose the apparatus parameters given in Table III.

TABLE III

| | |
|---|---|
| $A = 4.9 \cdot 10^{-2}$ cm$^2$ | Cross section of 2.5 mm dia. laser beam |
| $L = 12$ cm | Cell length |
| $n = 3.53 \cdot 10^{18}$ cm$^{-3}$ | Molecular density at 100 Torr |
| $h\nu_{12} = 4.13 \cdot 10^{-20}$ J | Photon energy of the P(14) transition at 2086.3 cm$^{-1}$ |
| $E_1 = 0.796 \cdot 10^{-20}$ J | Energy of CO state ($v = 0$, $J = 14$) |
| $\tau_{E_2} = 0.30$ sec | Time constant of decay for $v = 1$ states due to radiation in $CO/N_2$ |
| $J = 14$ | Rotational quantum number of $E_1$ |

When introduced into Eq. (9), the values of Table III determine the following power requirements:

At $T = 300$ K, with $k = 1.38 \cdot 10^{-23}$ J/K, P = 237 mW represents the instantaneous required power at the start of excitation. Under adiabatic conditions, the temperature begins to fall and, according to Eq. (9), the demand for power lessens. For example, as the temperature reaches 120 K, the required power is only 52 mW. After a few seconds, the asymptotic trend of the temperature is reached and the power demand approaches very small values. In this description, it has been assumed that the rates of events leading to cooling are much larger than those of heating due to such relaxation processes as VTR transfer and diffusion to and from the walls. The conclusion that the gas finally reaches a finite, although not vanishing, steady state temperature is in fact based on the existence of these losses.

The range of powers required for $CO/N_2$ is well within the rating of the SHG crystal. Similar evaluations have been performed for P-line pumping of CO. The difference between the two gases is that the radiative channel of nonthermal relaxation is ten times as fast in pure CO than in $CO/N_2$ (since in the former, every molecule has a dipole moment, rather than one in ten as in the latter). While this factor tends to increase the power requirement according to Eq. (9), it is compensated by a statistical weight factor which reduces $n_p$, as a detailed calculation shows. The power requirements are thus of the same order as in $CO/N_2$.

The parameters listed in Table III for the gas kinetic reaction cell were of course chosen beforehand so as not to exceed the available power rating of the laser system.

## 5.2 Diffusion Losses and Cell Diameter

When a vibrationally excited molecule drifts to and collides with a wall of the container, it has a certain probability of deactivation to the vibrational ground state. However, the detailed energy transfer processes do not appear to be known. There are four types of interactions possible which, in the order of their estimated probabilities, are the following:

(1) No transfer of vibrational energy.

(2) Transfer of vibrational energy to lattice phonons of wall; return of molecule with kT corresponding to wall temperature.

(3) Transfer of all or part of vibrational energy to R-T energy of molecule.

(4) Induced photon emission of photon of average energy $h\nu_{20}$.

Of these, the third mechanism is the most damaging since it returns in the average the vibrational energy $h\nu_{02}$, which is five times the rotational energy (see Table III), to the RT reservoir of the gas. In the event of alternatives (2) or (4), nothing is added to the energy balance that would not have occurred, if the molecule had previously returned to the ground state by radiation. The first process acts as if the cell diameter had been extended.

Experiments on the cooling balance in the low pressure regime should yield information on the probability of the third process. Nevertheless, to ensure conditions under which the effect of wall quenching is negligible, the diffusion time to and from the walls should be made long compared to the time of radiative relaxation.

Because of the importance of this problem, we calculated the required diameter of the cell in two ways. The first was a simple random walk calculation. In random walk, the average distance R reached after m steps of length $\Lambda$ equals $m^{1/2}\Lambda$. In gases $\Lambda$ represents the mean free path which is traversed in the collision time $\Lambda/\bar{v}$ at the mean velocity $\bar{v}$. The mean diffusion time to a distance R is therefore

$$t_{diff} = m \frac{\Lambda}{\bar{v}} = \frac{R^2}{\Lambda \bar{v}} \qquad (10)$$

which is (for mean free paths short compared to cell dimensions) proportional to the gas density n ($cm^{-3}$), but behaves as $T^{-1/2}$ at constant density and as $T^{-3/2}$ at constant pressure. At T = 273 K and 100 Torr, CO molecules have a mean velocity of $\bar{v} = 4.54 \cdot 10^4$ cm/sec and a mean free path $\Lambda = 4.91 \cdot 10^{-5}$ cm. Thus for CO at 100 Torr, 273 K:

$$t_{diff} = 0.45\ R^2 \quad . \qquad (11)$$

The second calculation used classical diffusion equations and published values[26] for the self-diffusion coefficients $D_{jj}$ of CO and $N_2$ ($D_{CO/CO} = 0.170$ and $D_{N_2/N_2} = 0.154$ cm$^2$ sec$^{-1}$ at T = 273 and 1 atm). This calculation showed that 32% of CO molecules at 100 Torr and 273 K had exceeded a range R after a time

$$t_{32\%} = 0.39\ R^2 \qquad (12)$$

with 10% longer delays for $N_2$.

These results led to the conclusion that a cell of at least 2 cm inner diameter produced a sufficiently long diffusion time over a path length R = 3 cm to the wall and back to the irradiated core. With a radiative relaxation time of 0.03 sec for pure CO and 0.3 sec for a 10% mixture of CO, only 7.7% of CO and $N_2$ molecules arrive at the wall in the average from the mixture at 100 Torr in a vibrationally excited state. For the case of pure CO, only $10^{-16}$ of the excited molecules hit the walls with their original vibrational energy still intact.

## 5.3 Design and Preparation of the Gas Reaction Cell

The considerations detailed in the two preceding sections led to the cell design shown in Fig. 4. It consists of a 5" long, 1" O.D. copper tube to which sapphire windows were brazed via flanges consisting of 70% Ni and 30% Fe. The completed window seal assemblies were obtained from Ceramaseal, Inc. The inside of the copper cylinder was painted with Aquadag, a product of Acheson Colloids Co., consisting of graphite suspended in water with a binding material. After heating above 450°C, which occurs conveniently during the brazing operations in an atmosphere of hydrogen, the graphite forms a black coating which is more than 95% absorbing for radiation at 5 μm. The purpose of the black layer is to prevent multiple reflections of the spontaneously emitted radiation from the copper wall. This radiation undergoes a certain amount of resonance

imprisonment, i.e., repeated processes of absorption (at somewhat lower cross sections than in the center of the line) and reemission. While these processes as such do not contribute to heating in the average, they prolong in effect the radiative lifetime of the vibrational states in the environment of the irradiated core (the core itself is relatively transparent, however, because of its near saturation.)

Tests showed that Aquadag withstood repeated heat treating cycles for vacuum outgassing without deterioration. Other blacks, such as CuO, were not considered to be as reliable.

Before the choice of black walls, the alternative of letting the radiation escape through the wall had not been overlooked. One-inch diameter sapphire tubes (polycrystalline transparent alumina) are, in fact, used by Westinghouse for arc lamps. Such a cell would permit steady state cooling of the structure itself, and the concept represents one of the embodiments of isothermal cooling by laser radiation. However, the need for four sealing operations (to two windows, the dynamic pressure gauge, and the pump line) did not appear warranted for the adiabatic cooling experiments.

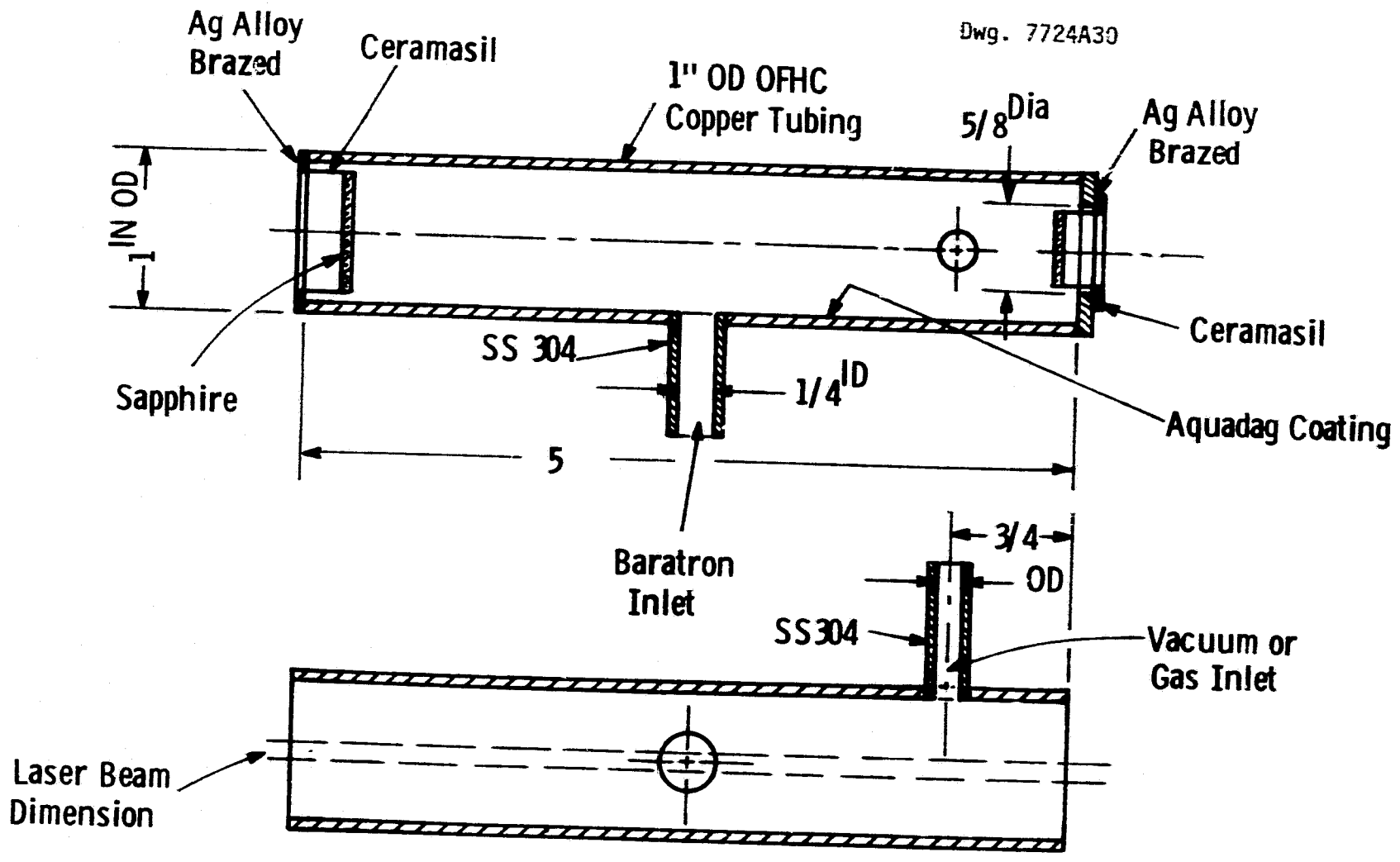


Fig. 4. Design of gas reaction cell with laser beam dimensions.

## 6. GAS HANDLING SYSTEM AND ASSEMBLY

### 6.1 Requirements of Gas Purity

The very small VRT collision rates of CO, $CO/N_2$, and $CO/N_2/He$ (the latter pertinent for isothermal cooling and other conditions) are possible only at high purities. This is especially true with respect to polyatomic gases, such as $H_2O$, $CO_2$, and hydrocarbons some of which have VRT rates $10^5$-$10^6$ times larger than CO. They should therefore not be present in concentrations larger than 1-0.1 ppm. We obtained from Matheson Gas Products Co. several one-liter glass flasks each of 99.99% pure CO and 99.998% pure $N_2$ (Research Grade). For CO the specified impurities were less than 100 ppm $N_2$, 20 ppm $O_2$, 200 ppm A, 10 ppm $CO_2$, 10 ppm $H_2$, and 2 ppm $C_xH_y$. Taking into account the known or estimated VRT rate of each component, these specified limits of impurity are still acceptable. The presence of a liquid nitrogen trap constitutes an additional safeguard (CO has, at nitrogen temperatures, still a vapor pressure of about 400 Torr).

Impurities other than those of the gas sources have to be minimized by preceding the filling of the cell with evacuation and bake-out cycles. A vacuum condition of $10^{-6}$ Torr is adequate since it contributes to a gas admitted at 100 Torr impurities of no more than 0.01 ppm. Bake-out cycles must be repeatable and must be performed on the installed system connected to the diffusion pump. The one-liter glass flasks, unlike steel tanks with differential pressure gauges, can be easily outgassed, but have to be replaced after about 20 filling operations.

### 6.2 System Assembly

The assembled system is shown in Fig. 5 (not to scale to emphasize certain details regardless of their size). The subassembly of the gas

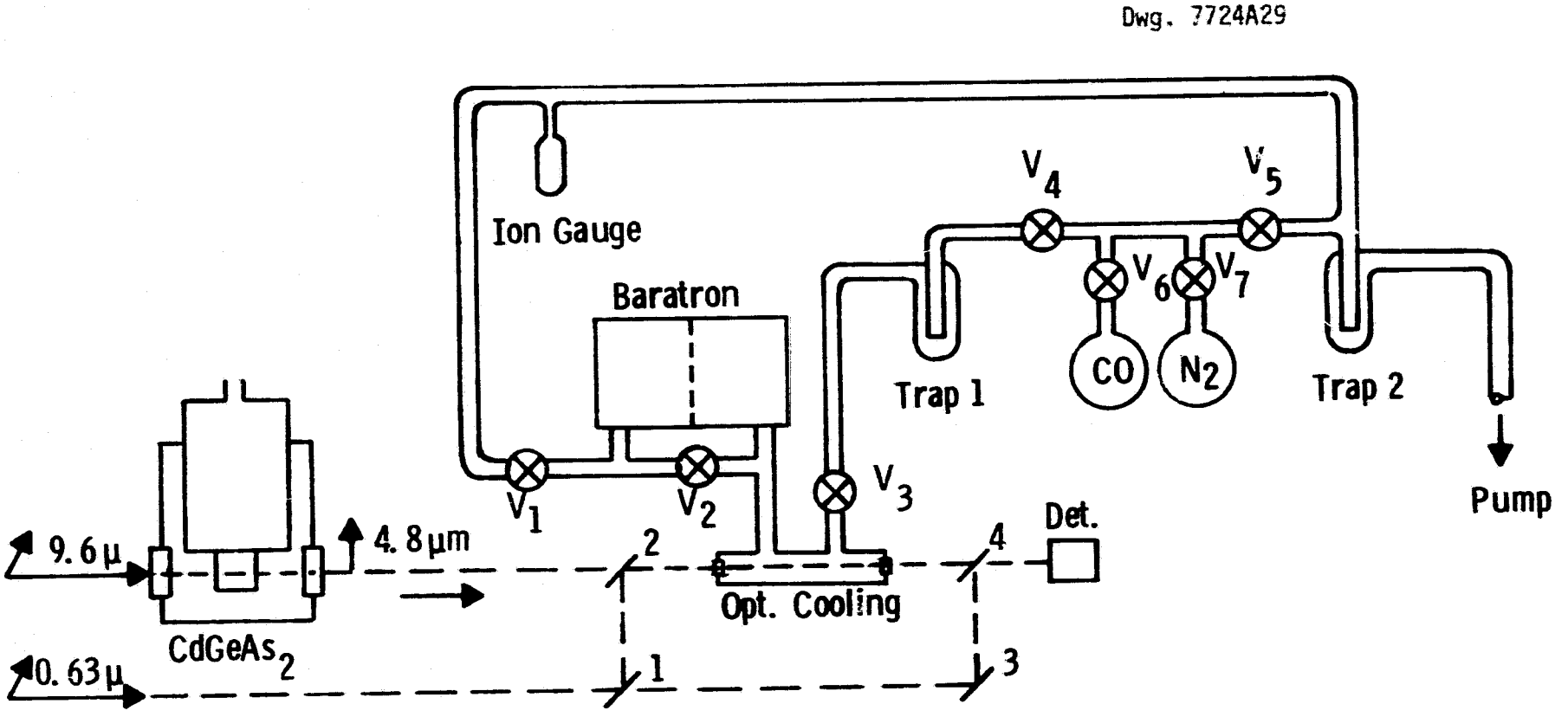


Fig. 5. Schematic diagram of the experimental system.

reaction cell between valves $V_1$ and $V_3$ uses stainless steel tubes of 1/4" outer diameter, 1/4" T-joints, Cajon seals to the Baratron pressure gauge, and stainless steel Nupro valves, all connected by brazing operations. Valves $V_2$ and $V_3$, when closed, isolate a gas volume which changes pressure in response to the resonance defect excitation. Since the adiabatic heat withdrawal is measured by the reduction of pressure, all "dead" volume outside the cell should be kept to a minimum. The volume of the gas cell itself is about 50 $cm^3$ whereas the volume in the tubing and the measurement compartment of the Baratron add up to about 7 $cm^3$. The reaction cell occupies therefore 88% of the volume isolated between valves $V_2$ and $V_3$.

To allow a sufficient pumping speed, the tubing outside of valves $V_1$ and $V_3$ is made of glass with 5/8" to 1" diameter except for the section between the Nupro valves $V_4$ and $V_5$. Because of the bake-out requirement, only stainless steel valves can be used. The volumes between $V_4$ and $V_5$ and between $V_3$ and $V_5$ represent gas sluices to meter out the desired CO or $N_2$ pressures to the gas cell and, by alternatively opening and closing valve $V_2$, also to the reference compartment of the Baratron between $V_1$ and $V_2$. Liquid nitrogen trap 2 conditions the vacuum outside valves $V_1$ and $V_5$. Trap 1 is operated during gas filling operations.

The entire gas handling and evacuation system is permanently wrapped by about 100' of heating tape consisting of insulated Cr-Ni strip. This permits repeated bake-out cycles during the course of experimentation.

## 6.3 Measurement Equipment

The phenomena that we expect to measure are of the following type and sequence in time t after the onset of continuous or pulsed radiation at t = 0 (100 Torr CO or $CO/N_2$):

(1) At t = 1 nsec, the molecules which have already undergone resonance defect transitions have mostly thermalized with the surrounding T/R heat reservoir. However, their density in the irradiated core has

not had time to change, and the small temperature reduction can only be measured by picosecond or nanosecond spectroscopy.

(2) At t = 1 μsec, the density in the core has begun to increase (this has occurred over a radial distance of about 0.5 mm with the speed of sound). Another effect,[8] not specifically mentioned in Section 3, that of further fast cooling by V-V escalation has also begun to take effect.

(3) At t = 1 msec, the pressure reduction in the cell begins to be sensed by the Baratron.

(4) At t = 100 msec, pure CO has gone through three cycles of spontaneous emission and repeated excitation, whereas $CO/N_2$ has just started to do so. Cooling has spread by diffusion to a radius of about 2.5 mm.

(5) At t = 3 sec, the pressure and the radial distributions of temperature and density, are approaching a steady state. The temperature at the steady state has a minimum in the core and results as the balance of defect cooling and VRT heating. Most of the VRT generated heat, however, is transported to the wall by radiation and there absorbed. Because of the high thermal conductivity of the copper enclosure, inside and outside surfaces of the wall are virtually at the same temperature, which is held constant by the environment. The radial temperature distribution thus varies from the minimum in the core to the wall temperature, typically at 300 K. The net heat content of the volume in the cell is reduced from the initial state by an amount which is measured as a pressure reduction at constant volume by the Baratron.

The events of this scenario are measured by two types of instrumentation:

(1) The Mach-Zehnder Arrangement shown in Fig. 5 measures the temperature in the core by its molecular density. The heart of the arrangement is the set of four beam splitters (1) to (4) shown in the figure. The beam from a Model 120 Spectra Physics He-Ne laser emerges polarized horizontally. Half of this beam is split towards a $CaF_2$ (or LiF) flat (2) so that, at its horizontal polarization, about 5% of it is transmitted through the axis of the cell. The other half of the beam traverses the

coated silica beam splitter (1) and is reflected by Au mirror (3) towards a second $CaF_2$ flat (4). At this beam splitter, the two halves of the He-Ne beam are superposed with equal intensity, corrected by a neutral filter and focused on a pinhole in front of a photomultiplier. The frequency doubled $CO_2$ laser beam is made collinear with the He-Ne laser beam by beam splitter (2).

The measurement sensitivity of changes in density and temperature can be estimated on the basis of the refraction indices for CO ($n = 1.000044$ at 100 Torr and 300 K) and $N_2$ ($n = 1.000039$ at 100 Torr and 300 K). The 12 cm length of the cell produces at 100 Torr a path length which is increased over that of vacuum by 8.9 $\lambda$ and 7.3 $\lambda$, respectively, for the wavelength $\lambda = 6.3 \cdot 10^{-5}$ cm of He-Ne. The thermally caused increase of the optical path length in the cell amounts to about 0.025 $\lambda$/K. Starting with complete destructive interference of the two superposed beams, 0.1 K represents the mirimum detectable temperature change, if sufficiently stable beam conditions are obtained.

Used with an oscilloscope of appropriate speed, the Mach-Zehnder arrangement can follow the dynamic temperature behavior from time scales of 100 nsec on upward.

(2) The Baratron (MKS Instruments, Inc.) has a dynamic range of pressure measurement of 10 Torr. The reference side of the gauge must therefore be first raised to the appropriate bias pressure. The specified accuracy at full scale is 0.08%. If initially at 100 Torr and 300 K, the gas temperature in the cell has to change 30 K to produce a full scale response and is measured with an accuracy of 0.024 K. The accuracy is still much higher, according to the manufacturer's specifications, at fractional scale readings.

Because the Baratron gauge operates by the capacitive sensing of a deflection produced in a diaphragm, its minimum response time is only 2 msec. According to Eqs. (11) or (12), cooling has spread beyond the core after 2 msec only to a fraction of a millimeter. The pressure change measured by the gauge is, therefore, caused by the temperature change of the core, subject to a small correction. Typically, such a measurement is started by equalizing the pressure of the two Baratron

compartments via valve $V_2$. To gain an impression of the accuracy possible, assume initial conditions of 300K, 100 Torr. A temperature change of 0.3 K then causes in the core a fractional density change of $1 \cdot 10^{-3}$ and $1 \cdot 10^{-5}$ in the cell. The measurement side of the baratron thus experiences an increase by $1 \cdot 10^{-3}$ Torr which, according to MKS graphs, it reads with 1% accuracy. Hence, the 0.3 K temperature change in the core is measured to an accuracy of 0.003 K.

Because of the linear relationship between pressure and temperature at constant volume, the gauge measures the difference in the heat content of the gas volume in the cell at the start of radiation and at times up to the steady state condition. It is possible to calculate from this the temperature that has been reached in the core. More important, one can determine the temperature that would be reached, under otherwise equal conditions in an irradiated gas core of a diameter large compared to the mean diffusion range at the time of the steady state condition (note that, because of molecular level saturation, that temperature is <u>not</u> obtained by merely multiplying the mean temperature drop of the cell volume by the cross section ratio of cell and core).

## 7. PLANNED AND PROPOSED EXPERIMENTS AND MEASUREMENTS

At the present work status, the assembled system is ready for the measurement phase. The experiments which were planned under this contract were to explore adiabatic cooling. In detail, they were the following:

(1) Measurement of the gas temperature as a function of time from milliseconds to seconds at various pressures from 1 Torr to about 300 Torr of pure CO. The experiments were to be performed with 2.5 mm diameter laser beams, but comparison experiments with 5 mm beams were also planned.

(2) Measurements of the same type as under (1) on $CO/N_2$. Mixtures of 10 and 50 Torr CO each at various added pressures of nitrogen were to be investigated, the choice to some extent depending on (1).

(3) Investigation of the gas kinetic transfer phenomena in the time domain from the shortest time achievable with the system in pulsed operation to milliseconds. These are essentially operations at low energy in which density and pressure changes are measured simultaneously. Some of these measurements were also to be taken with long pulses and higher total energy input from milliseconds to seconds.

These measurements were intended to determine the magnitude and time behavior of the temperature in the core and, indirectly with further analysis and calibration, of the radial temperature distribution in the gas kinetic reaction cell. The variation of the experimental parameters has as a main objective the assessment of competing transfer processes and their effect on adiabatic cooling. These are, in the order of their respective relaxation times at intermediate pressures, the following: VV energy transfer, resonance imprisonment, diffusion to the walls, and VRT thermal relaxation.

Aside from exploring laser induced heat pump processes as such, the experiments and measurements outlined here are expected to yield

compartments via valve $V_2$. To gain an impression of the accuracy possible, assume initial conditions of 300 K, 100 Torr. A temperature change of 0.3 K then causes in the core a fractional density change of $1 \cdot 10^{-3}$ and $1 \cdot 10^{-5}$ in the cell. The measurement side of the baratron thus experiences an increase by $1 \cdot 10^{-3}$ Torr which, according to MKS graphs, it reads with 1% accuracy. Hence, the 0.3 K temperature change in the core is measured to an accuracy of 0.003 K.

Because of the linear relationship between pressure and temperature at constant volume, the gauge measures the difference in the heat content of the gas volume in the cell at the start of radiation and at times up to the steady state condition. It is possible to calculate from this the temperature that has been reached in the core. More important, one can determine the temperature that would be reached, under otherwise equal conditions in an irradiated gas core of a diameter large compared to the mean diffusion range at the time of the steady state condition (note that, because of molecular level saturation, that temperature is <u>not</u> obtained by merely multiplying the mean temperature drop of the cell volume by the cross section ratio of cell and core).

## 7. PLANNED AND PROPOSED EXPERIMENTS AND MEASUREMENTS

At the present work status, the assembled system is ready for the measurement phase. The experiments which were planned under this contract were to explore adiabatic cooling. In detail, they were the following:

(1) Measurement of the gas temperature as a function of time from milliseconds to seconds at various pressures from 1 Torr to about 300 Torr of pure CO. The experiments were to be performed with 2.5 mm diameter laser beams, but comparison experiments with 5 mm beams were also planned.

(2) Measurements of the same type as under (1) on $CO/N_2$. Mixtures of 10 and 50 Torr CO each at various added pressures of nitrogen were to be investigated, the choice to some extent depending on (1).

(3) Investigation of the gas kinetic transfer phenomena in the time domain from the shortest time achievable with the system in pulsed operation to milliseconds. These are essentially operations at low energy in which density and pressure changes are measured simultaneously. Some of these measurements were also to be taken with long pulses and higher total energy input from milliseconds to seconds.

These measurements were intended to determine the magnitude and time behavior of the temperature in the core and, indirectly with further analysis and calibration, of the radial temperature distribution in the gas kinetic reaction cell. The variation of the experimental parameters has as a main objective the assessment of competing transfer processes and their effect on adiabatic cooling. These are, in the order of their respective relaxation times at intermediate pressures, the following: VV energy transfer, resonance imprisonment, diffusion to the walls, and VRT thermal relaxation.

Aside from exploring laser induced heat pump processes as such, the experiments and measurements outlined here are expected to yield

information on gas kinetic coefficients by methods different, and often not obtainable, from a spectroscopic approach. This includes collisional energy transfer rates, especially those involving molecules without an electric dipole moment, and the relatively unexplored conversion of vibrational energy in collision with walls. Such experiments, which may quite possibly encounter impasses and phenomena not foreseen by us, may prove of value to such other fields as chemistry and isotope separation induced by lasers, as well as to the development of gas lasers themselves.

## ACKNOWLEDGMENTS

The technical monitor of this contract was Dr. K. Billman until he left for EPRI. We wish to thank him for his continued help and encouragement. We also express our thanks to Dr. A. Mooradian and Dr. N. Menyuk of the MIT Lincoln Laboratory for the loan of a $CdGeAs_2$ crystal.

This report has been typed by M. Fischer.

## REFERENCES


1. (a) Laser Engines Operating by Resonance Absorption, NASA-Ames Contract NAS2-8372.
   (b) M. Garbuny, Laser Energy Conversion Symposium, K. W. Billman, ed., NASA-Ames, 18-19 January 1973, NASA TM X-62,269.

2. (a) M. Garbuny and M. J. Pechersky, Second Laser Energy Conversion Symposium, K. W. Billman, ed., NASA-Ames, 27-28 January 1975, NASA SP-395.
   (b) M. Garbuny and M. J. Pechersky, Final Report, Contract NAS2-8372.
   (c) M. Garbuny and M. J. Pechersky, Appl. Opt. 15, 1141 (1976).

3. (a) R. L. Byer, Laser Energy Conversion Symposium, K. W. Billman, ed., NASA-Ames, 18-19 January 1973.
   (b) K. W. Billman, Astronaut. Aeronaut., 13 56 (1975).
   (c) G. Lee, private communication.

4. W. R. Martini, "Space Electric Power Design Study," Report A-29674-B(DG), NASA-Ames Research Center.

5. R. T. Taussig, P. E. Cassidy and E. Zumdieck in "Radiation Energy Conversion in Space", K. W. Billman, ed., Progress in Astronautics and Aeronautics, Vol. 61.

6. (a) W. H. Christiansen and A. Hertzberg, Proc. IEEE 61, 1060 (1973).
   (b) M. Garbuny, Optics Comm. 18, 77 (1976).

7. "Isentropic Processes for Laser Engines", NASA-Ames Contract NAS2-9185.

8. M. Garbuny, Final Report NAS2-9185; also J. Chem. Phys. 67, 5676 (1977).

9. T. W. Haensch and A. L. Schowlow, Opt. Commun. 13, 68 (1975).

10. W. Neuhauser, M. Hohenstatt, P. Toschek, and H. Dehmelt, Phys. Rev. Lett. 41, 233 (1978).

11. D. J. Wineland, R. E. Drullinger, and F. L. Walls, Phys. Rev. Lett. 40, 1639 (1978).

12. R.C.C. Leite, S.P.S. Porto, and T. C. Damon, Appl. Phys. Lett. 10, 100 (1967).

13. F. G. Gebhardt and D. C. Smith, Appl. Phys. Lett., 20, 129 (1972).

14. See e.g., M. Garbuny, "Optical Physics", Academic Press (1965).

15. G. Herzberg, "Molecular Spectra and Molecular Structure", Vol. I, "Spectra of Diatomic Molecules", 2nd Ed., Van Nostrand Reinhold (1950).

16. J. P. Bouanich and C. Brudbeck, J. Quant. Spec. Rad. Trans. 13, 1 (1973).

17. A. E. Greene and R. A. Harris, J. Appl. Phys. 46, 5039 (1975).

18. K. W. Nill, F. A. Blum, A. R. Calava, and T. C. Harman, Appl. Phys. Lett. 19, 79 (1971).

19. H. Kildal and R. L. Byer, Proc. IEEE 59, 1644 (1971).

20. R. Beck, W. English, and K. Gürs, Table of Laser Lines in Gases and Vapors, 2nd Ed., Springer (1978).

21. N. Djeu, Appl. Phys. Lett. 23, 309 (1973).

22. H. Kildal and T. F. Deutsch, "Optically Pumped Gas Lasers" in Tunable Lasers and Applications, A. M. Mooradian, et al., eds., Springer (1976).

23. A.H.M. Ross, R. S. Eng and H. Kildal, Optics Commun. 12, 433 (1974).

24. R. K. Kao, C. J. Humphreys and D. H. Rank, Wavelength Standards in the Infrared, Academic Press (1966).

25. M. Garbuny, in "Coherence and Quantum Optics IV, L. Mandel and E. Wolf, eds., Plenum (1978).

26. Landolt-Bornstein, "Zahlenwerk und Funktionen", 6th ed., Vol. II, Part Va, "Transport Phenomena", p. 516, Springer (1969).